



**HAL**  
open science

# $\alpha$ II- $\beta$ V spectrin bridges the plasma membrane and cortical lattice in the lateral wall of the auditory outer hair cells

Kirian Legendre, Saaïd Safieddine, Polonca Küssel-Andermann, Christine Petit, Aziz El-Amraoui

► **To cite this version:**

Kirian Legendre, Saaïd Safieddine, Polonca Küssel-Andermann, Christine Petit, Aziz El-Amraoui.  $\alpha$ II- $\beta$ V spectrin bridges the plasma membrane and cortical lattice in the lateral wall of the auditory outer hair cells. *Journal of Cell Science*, 2008, 121 (20), pp.3347-3356. 10.1242/jcs.028134 . pasteur-03926801

**HAL Id: pasteur-03926801**

**<https://pasteur.hal.science/pasteur-03926801>**

Submitted on 6 Jan 2023

**HAL** is a multi-disciplinary open access archive for the deposit and dissemination of scientific research documents, whether they are published or not. The documents may come from teaching and research institutions in France or abroad, or from public or private research centers.

L'archive ouverte pluridisciplinaire **HAL**, est destinée au dépôt et à la diffusion de documents scientifiques de niveau recherche, publiés ou non, émanant des établissements d'enseignement et de recherche français ou étrangers, des laboratoires publics ou privés.

Copyright

# $\alpha$ II- $\beta$ V spectrin bridges the plasma membrane and cortical lattice in the lateral wall of the auditory outer hair cells

Kirian Legendre<sup>1,2,3</sup>, Saaid Safieddine<sup>1,2,3</sup>, Polonca Küssel-Andermann<sup>1</sup>, Christine Petit<sup>1,2,3</sup> and Aziz El-Amraoui<sup>1,2,3,\*</sup>

<sup>1</sup>Institut Pasteur, Unité de Génétique et Physiologie de l'Audition, 25 rue du Dr Roux, 75015 Paris, France

<sup>2</sup>INSERM UMRS587, F75015 Paris, France

<sup>3</sup>UPMC Paris 06, F75015 Paris, France

\*Author for correspondence (e-mail: aziz.el-amraoui@pasteur.fr)

Accepted 21 July 2008

Journal of Cell Science 121, 3347-3356 Published by The Company of Biologists 2008

doi:10.1242/jcs.028134

## Summary

The sensitivity and frequency selectivity of the mammalian cochlea involves a mechanical amplification process called electromotility, which requires prestin-dependent length changes of the outer hair cell (OHC) lateral wall in response to changes in membrane electric potential. The cortical lattice, the highly organized cytoskeleton underlying the OHC lateral plasma membrane, is made up of F-actin and spectrin. Here, we show that  $\alpha$ II and two of the five  $\beta$ -spectrin subunits,  $\beta$ II and  $\beta$ V, are present in OHCs.  $\beta$ II spectrin is restricted to the cuticular plate, a dense apical network of actin filaments, whereas  $\beta$ V spectrin is concentrated at the cortical lattice. Moreover, we show that  $\alpha$ II- $\beta$ V spectrin directly interacts with F-actin and band 4.1, two components of the OHC cortical lattice.  $\beta$ V spectrin is progressively recruited into the cortical lattice between postnatal day 2 (P2) and P10 in the mouse, in parallel with prestin membrane insertion, which itself parallels

the maturation of cell electromotility. Although  $\beta$ V spectrin does not directly interact with prestin, we found that addition of lysates derived from mature auditory organs, but not from the brain or liver, enables  $\beta$ V spectrin–prestlin interaction. Using this assay,  $\beta$ V spectrin, via its PH domain, indirectly interacts with the C-terminal cytodomain of prestin. We conclude that the cortical network involved in the sound-induced electromotility of OHCs contains  $\alpha$ II- $\beta$ V spectrin, and not the conventional  $\alpha$ II- $\beta$ II spectrin.

Supplementary material available online at  
<http://jcs.biologists.org/cgi/content/full/121/20/3347/DC1>

Key words:  $\beta$ V spectrin, Prestin, Outer hair cell, Cortical lattice, Electromotility

## Introduction

Among species, the mechanosensory hair cells of the inner ear share many structural and functional features, including a force-producing mechanism in the hair bundle that is proposed to be involved in the amplification of sound or of acceleration mechanical stimuli (Fettiplace, 2006). Mammals have also evolved an additional mechanical amplification process, called electromotility, which is unique to the outer hair cells (OHCs) of their auditory sense organ, the cochlea (supplementary material Fig. S1). Electromotility consists of voltage-dependent-contraction and -elongation cycles of the OHC lateral wall, which are synchronized with sound stimulation (Brownell et al., 1985). The changes in OHC length are driven by changes in the conformation of the integral membrane protein prestin (Zheng et al., 2000) – a member of the solute-carrier family SLC26A – which is abundant in the lateral plasma membrane of these cells (Belyantseva et al., 2000). Targeted deletion of the gene encoding prestin (*SLC26A5*) in mouse abolishes electromotility and the frequency selectivity of the cochlear response, and results in a significant (~60 dB) loss of cochlear sensitivity (Liberman et al., 2002). Because OHCs of prestin-knockout mice have significantly altered mechanical properties [OHC length and stiffness, mechano-electrical transducer (MET) currents], the real contribution of electromotility to cochlear amplification has been a matter of debate (Chan and Hudspeth, 2005). Recently, a prestin-

knockin mouse was engineered in which two amino acid residues at the junction between the last transmembrane domain and the intracellular C terminus were replaced (V499G/Y501H) (Dallos et al., 2008). Despite normal MET currents and organ-of-Corti mechanics, these mice display knockout-like behavior, unequivocally demonstrating that prestin-driven electromotility is a necessary condition for sound amplification (Dallos et al., 2008). The OHC is a cylindrical hydrostat, the shape of which is maintained by a pressurized fluid core and a highly organized and mechanically reinforced lateral wall. The latter forms a unique trilaminar structure (100-nm thick) that consists of the plasma membrane, cortical lattice and innermost membranous lateral system, forming 'subsurface cisternae' (Ashmore, 2008; Brownell et al., 2001) (supplementary material Fig. S1). Electron-microscopy studies have shown that the cortical lattice consists of circumferential filaments, 5–8 nm in diameter, that are cross-linked with filaments that are 2–4 nm in diameter (Holley and Ashmore, 1988; Holley et al., 1992). From immunolabeling studies, it has been proposed that these filaments are composed of actin and spectrin, respectively (Holley and Ashmore, 1990; Mahendrasingam et al., 1998). Pillars (25 nm in length), of unknown molecular composition, connect the cortical lattice to the plasma membrane throughout the OHC lateral wall (Holley et al., 1992). Disruption of the actin-spectrin association by diamide reduces OHC electromotility and cell longitudinal

stiffness (Adachi and Iwasa, 1997; Oghalai et al., 1998). In addition, inhibition of the small GTPase RhoA and its downstream target, the Rho-kinase ROCK, has been shown to decrease the OHC electromotile response (Zhang et al., 2003). Although the precise molecular mechanisms underlying these regulatory processes are still unknown, they point to a key role of the cytoskeleton in OHC electromotility (Adachi and Iwasa, 1997; Oghalai et al., 1998; Zhang et al., 2003).

A large number of experimental and theoretical studies devoted to the mechanical properties of the OHC lateral membrane (Brownell et al., 2001) have been based on the seminal studies on red-blood-cell cytomechanics (Discher and Carl, 2001). Similar to OHCs, red blood cells display a highly specialized two-dimensional spectrin-based membrane skeleton that is essential for the structural and mechanical properties of their plasma membrane. In mammals, two  $\alpha$ -spectrin subunits ( $\alpha$ I and  $\alpha$ II), four conventional  $\beta$ -spectrin subunits ( $\beta$ I to  $\beta$ IV) and a  $\beta$ -heavy subunit ( $\beta$ V) have been reported (De Matteis and Morrow, 2000). Red-blood-cell spectrin consists of  $\alpha$ I and  $\beta$ I subunits that are aligned side by side to form heterodimers, which assemble head to head in a tetrameric ( $\alpha$ ,  $\beta$ )<sub>2</sub> structure (De Matteis and Morrow, 2000; Dubreuil, 2006). By contrast, the precise composition of the spectrin-based network in the lateral wall of OHCs is still unknown. Even though immunolabeling has been observed along the OHC lateral wall by using antibodies directed against red-blood-cell heterodimeric spectrin (both  $\alpha$ I and  $\beta$ I subunits), it was since assumed that the non-erythrocyte subunit  $\beta$ II (formerly known as fodrin) is present in the OHC cortical lattice (Holley and Ashmore, 1990; Knipper et al., 1995). In addition, a detailed analysis by immunogold electron microscopy has shown that an  $\alpha$ -spectrin subunit is present in the OHC cortical lattice (Mahendrasingam et al., 1998). We thus decided to reinvestigate the composition of the spectrin-based network in the OHC cortical lattice.

## Results

### Localization of the conventional spectrin subunits in the auditory organ

Combinatorial association of different  $\alpha$  and  $\beta$  spectrins yields heterotetramers that display distinct tissue-specific cellular and subcellular patterns of expression and function (De Matteis and Morrow, 2000; Dubreuil, 2006). In organ-of-Corti tissue samples dissected from postnatal day 10 (P10) mice, direct sequencing of reverse transcriptase (RT)-PCR products showed the presence of  $\alpha$ II spectrin and all the known  $\beta$ -spectrin isoforms ( $\beta$ I,  $\beta$ II,  $\beta$ III,  $\beta$ IV and  $\beta$ V) (Fig. 1A,B; supplementary material Table S1). We compared the cellular and subcellular distributions of the various spectrin subunits by immunofluorescence analysis using confocal microscopy. Antibodies that specifically recognize each of the four conventional  $\beta$ -spectrin subunits were used (see Materials and Methods) on whole mounts (Fig. 1C,D) and cross-sections (Fig. 2A-C) of the auditory epithelium as well as on isolated hair cells (Fig. 2F,H,I). As expected,  $\alpha$ II spectrin (see Mahendrasingam et al., 1998) (Fig. 1C,D and Fig. 2A) and  $\beta$ II spectrin (Fig. 1D and Fig. 2C) were widely distributed; they were detected in the auditory hair cells, and their supporting cells, as well as in the fibroblasts of the underlying connective tissue.  $\beta$ I-spectrin labeling could not be detected in the auditory sensory epithelium. Finally,  $\beta$ III spectrin was detected in the cell bodies of cochlear ganglion neurons, whereas  $\beta$ IV spectrin was observed at nodes of Ranvier along the auditory nerve fibers (supplementary material Fig. S2). Therefore, of the four conventional  $\beta$ -spectrin subunits, only  $\beta$ II was detected in auditory hair cells.

### $\beta$ V spectrin – the mammalian $\beta$ -heavy-spectrin subunit in the auditory organ

Similar to conventional  $\beta$ -spectrin subunits,  $\beta$ V spectrin has three distinct regions (Stabach and Morrow, 2000): an N-terminal region with two calponin homology (CH) motifs, a large central region composed of 30 spectrin repeat units (the 30th being partial) instead of the 17 repeats found in conventional  $\beta$  spectrins, and a C-terminal pleckstrin homology (PH)-domain-containing region (see Fig. 1A). To analyze the distribution of  $\beta$ V spectrin in the inner ear, we produced a polyclonal anti- $\beta$ V spectrin antibody against a C-terminal region of human  $\beta$ V spectrin (see Materials and Methods) (supplementary material Fig. S3). In the cochlear sensory epithelium of P10 mice,  $\beta$ V spectrin immunoreactivity was detected only in the hair cells. No labeling was detected in the supporting cells (Fig. 1E,F and Fig. 2D). In addition, a  $\beta$ V spectrin labeling of endothelial cells was present in the connective tissue of the cochlear spiral limbus (arrowheads in Fig. 1E) and lateral wall (supplementary material Fig. S4C), consistent with the results of RT-PCR experiments (supplementary material Fig. S4A-E). Confocal microscopy on whole mounts (Fig. 1E,F) and cross-sections (Fig. 2D) of the auditory epithelium revealed that  $\beta$ V spectrin is particularly abundant in OHCs (see also supplementary material Fig. S5A,B). The labeling extended all along the lateral wall, from just below the cuticular plate to the basal pole of the cell (Fig. 2D,G; supplementary material Fig. S6A). By contrast,  $\beta$ II-spectrin immunoreactivity predominated in the apical cuticular plate and was not detected along the lateral wall (Fig. 2H), whereas the  $\alpha$ II subunit was detected both in the cuticular plate and along the lateral wall (Fig. 2I; supplementary material Fig. S6B). Finally, immunofluorescence analysis of isolated inner hair cells (IHCs), the genuine sensory cells of the cochlea, showed a  $\beta$ V spectrin submembrane labeling, most prominent in the cell subapical region (neck region) (Fig. 2D,E; supplementary material Fig. S5 and Fig. S6A).

To localize  $\beta$ V spectrin at the ultrastructural level, we carried out post-embedding immunogold electron microscopy on sections of the organ of Corti from P15 mice. In all examined organs of Corti, the gold particles were mainly associated with the lateral wall of OHCs, but not with adjacent supporting cells (Fig. 3A-C). Little or no labeling was observed on the stereocilia, the cuticular plate, the apical junctional complex or other cytoplasmic regions of OHCs (Fig. 3A,D; supplementary material Fig. S7A,B). Quantitative analysis carried out on 17 different OHCs derived from three different mice showed that most of the gold particles ( $n=121$ ) were aligned along the lateral wall (79% of the gold particles), in agreement with the submembrane labeling obtained by immunohistofluorescence (Fig. 2). Only 4% of the particles were seen in the cuticular-plate region and 17% within the cytoplasm (supplementary material Fig. S7A,B).

### $\beta$ V spectrin directly interacts with $\alpha$ II spectrin, F-actin and band 4.1

The  $\alpha$ II- and  $\beta$ V spectrin subunits were colocalized in the OHC cortical lattice (Fig. 2G,I), which is consistent with their possible association to form spectrin heterodimers. Indeed, in pull-down assays, the GST-tagged  $\beta$ V29 fragment (which contains the C-terminal region of  $\beta$ V spectrin, starting at the spectrin Repeat 29; aa 3317-3674) bound to  $\alpha$ II spectrin from total-protein extracts of P8 mouse organs of Corti (Fig. 4A,B). The existence of  $\alpha$ II- $\beta$ V spectrin dimers in vivo was confirmed on the same tissue extracts by the co-immunoprecipitation of the  $\alpha$ II- and  $\beta$ V spectrin subunits with the anti- $\beta$ V spectrin antibody (Fig. 4C).

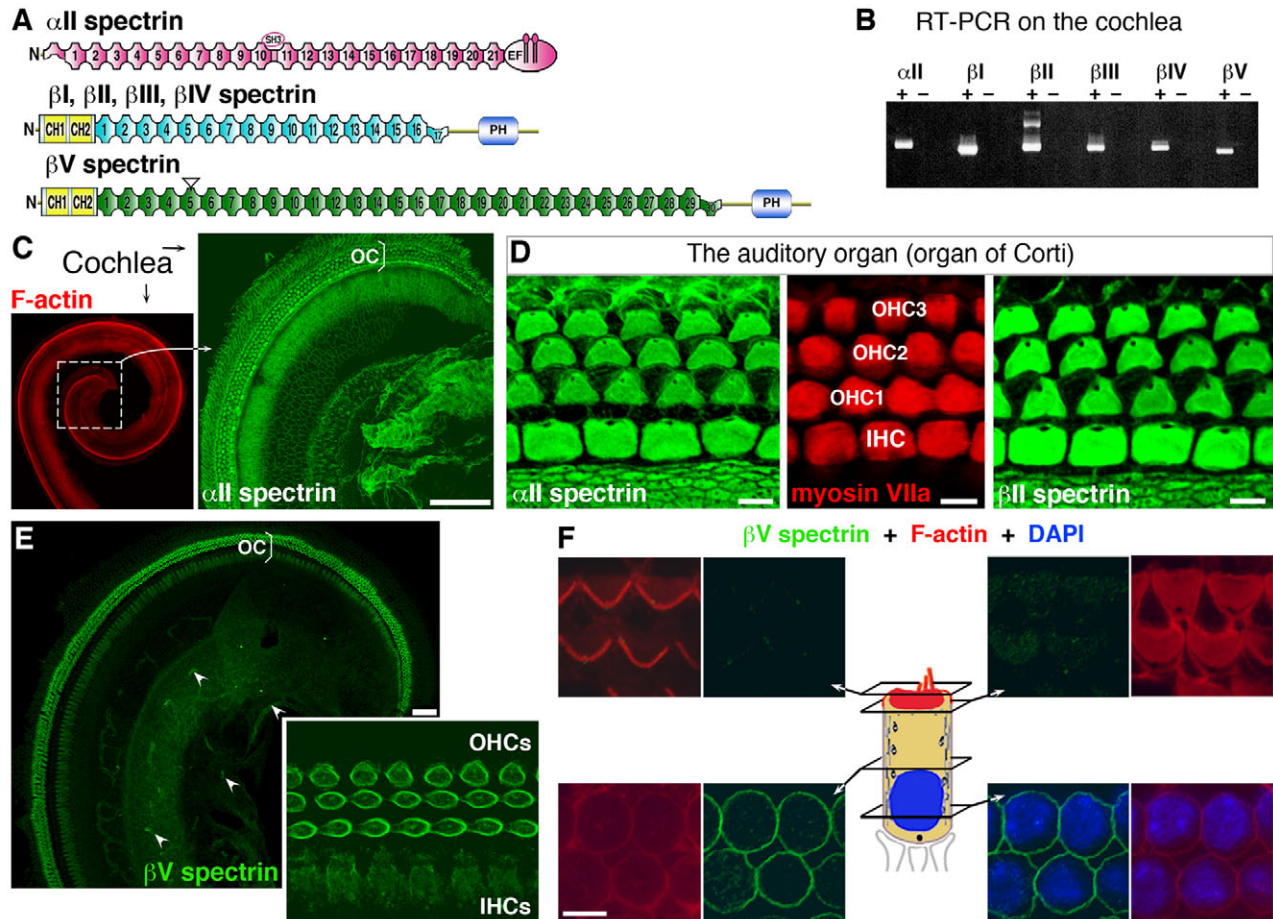


**Fig. 1.** Spectrin subunits in the auditory organ. (A) Spectrins exist as heterotetramers composed of  $\alpha$ - and  $\beta$ -spectrin subunits [ $(\alpha, \beta)_2$ ]. The  $\alpha$  and  $\beta$  subunits present the same structural modular organization, mainly made up of multiple triple-helical repeat units: 21 for  $\alpha$  subunits, 17 for conventional  $\beta$  subunits and 30 for  $\beta$ V. Other domains, such as the Src-homology domain (SH3) and the EF-hand calmodulin-binding domain in  $\alpha$ II spectrin, and the N-terminal calponin homology (CH) domains and C-terminal pleckstrin-homology (PH) domain in  $\beta$  spectrins, are indicated. (B) RT-PCR analysis on mouse organ-of-Corti tissue samples at P10 shows the presence of transcripts encoding the  $\alpha$ II-spectrin and all known  $\beta$ -spectrin subunits, i.e.  $\beta$ I,  $\beta$ II,  $\beta$ III,  $\beta$ IV and  $\beta$ V. (C-F) Whole mounts of organs of Corti (OC) from P8-P10 mice. Actin filaments (F-actin, red) are labeled with rhodamin-conjugated phalloidin. The  $\alpha$ II- and  $\beta$ II-spectrin subunits (green; C,D) are detected both in the sensory hair cells and their supporting cells. (E) By contrast, the  $\beta$ V spectrin subunit is detected in the sensory hair cells only. A strong  $\beta$ V spectrin labeling is observed in OHCs (see inset). (F) Serial confocal planes (0.6- $\mu$ m thick) at different levels of the OHC (see middle panel) show that  $\beta$ V spectrin is restricted to the cortical lattice, along the cell lateral wall. Scale bars: 50  $\mu$ m (C,E); 5  $\mu$ m (D,F).

The murine  $\beta$ V spectrin putative actin-binding region, the N-terminal CH domains ( $\beta$ VCH, aa 1-250), has 51% aa sequence identity with the corresponding region of  $\beta$ II spectrin. To determine whether  $\beta$ V spectrin actually binds to F-actin, we purified a GST-tagged  $\beta$ VCH fragment from *Escherichia coli* and carried out F-actin co-sedimentation assays. In the presence of F-actin, the bulk of the GST-tagged  $\beta$ VCH fusion protein co-sedimented with F-actin, whereas, in its absence, it remained in the supernatant (Fig. 4D). We conclude that  $\beta$ V spectrin directly interacts with F-actin.

In red blood cells, the interaction between spectrin and the plasma membrane inner layer has been reported to control the elasticity of the cell membrane, its biconcave shape, and also lipid and protein lateral diffusion in the plasma membrane (Markin and Kozlov, 1988). The plasma membrane and conventional spectrin-based cytoskeleton form two parallel sheets connected through interactions that involve two distinct molecular links (De Matteis and Morrow, 2000). One link involves the  $\beta$  spectrin R15 (Kennedy et al., 1991), ankyrin and band 3, whereas the other requires the spectrin N-terminal region, band 4.1R (EPB41) and glycophorin C (De Matteis

and Morrow, 2000; Dubreuil, 2006). The ankyrin-binding sequence that is well conserved among conventional  $\beta$  spectrins, however, is not present in  $\beta$ V spectrin (Stabach and Morrow, 2000). Other interactions might thus mediate  $\beta$ V spectrin association to the plasma membrane. We first tested whether  $\beta$ V spectrin is linked to the plasma membrane through a binding of its N-terminal region to band 4.1; this protein has been detected in the lateral wall of OHCs (Knipper et al., 1995; Zine and Schweitzer, 1997) and is thought to be a component of the pillars connecting the OHC lateral membrane to the cortical lattice. Unlike other FERM proteins, band 4.1 is able to bind concomitantly to F-actin and spectrin through its spectrin-actin binding (SAB) domain (Bretscher et al., 2002). In vitro binding experiments indeed showed that GST-tagged  $\beta$ VCH directly interacts with the SAB domain (aa 611-678) of band 4.1G (EPB41L2) (Fig. 4E). In addition, we carried out immunoprecipitation experiments with extracts of P8 mouse organs of Corti. The immunoprecipitates obtained with the anti- $\beta$ V spectrin antibodies did contain the two immunoreactive bands characteristic of the band 4.1 protein (Fig. 4F). We conclude that band 4.1 and

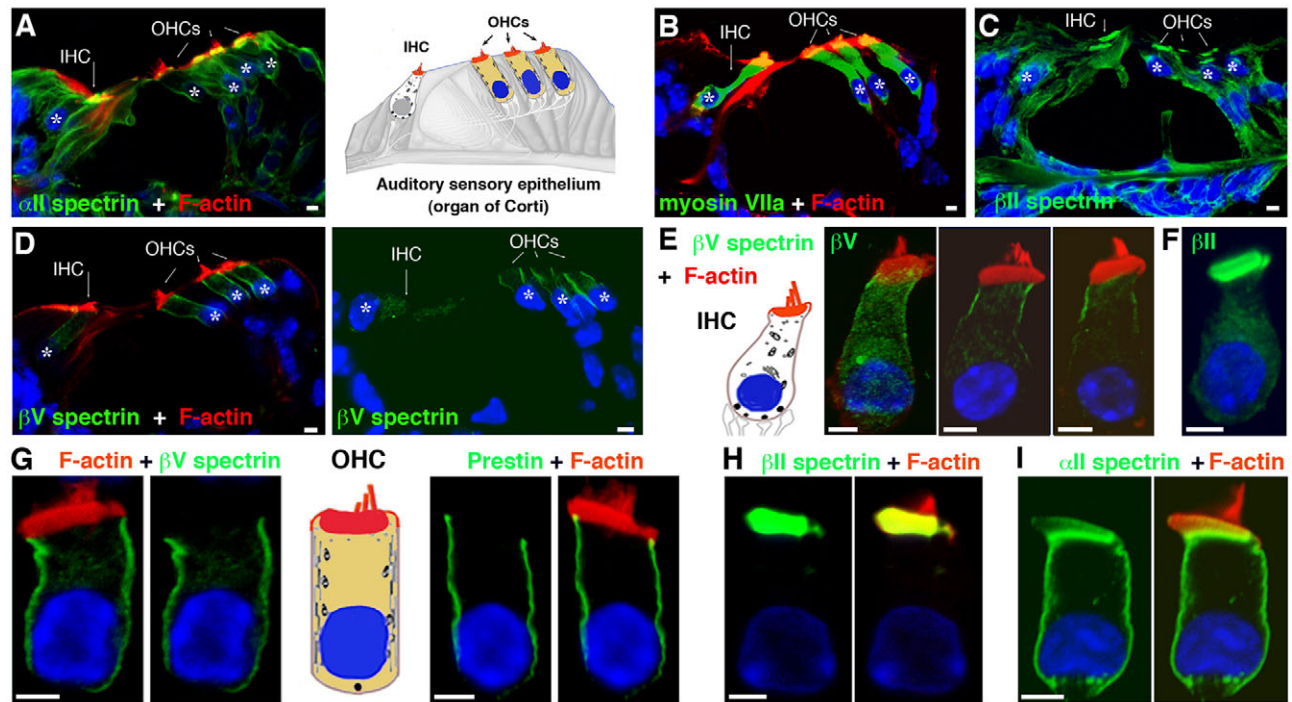


**Fig. 2.** Spectrin subunits are present in different subcellular regions in outer and inner hair cells. (A–D) Cross-sections through organs of Corti from P8–P10 mice. The mammalian cochlea contains two classes of hair cells: inner and outer hair cells (IHCs and OHCs, respectively; labeled with an anti-myosin-VIIa antibody, B). Whereas the  $\alpha$ II- and  $\beta$ II-spectrin subunits are detected in both types of hair cells and flanking supporting cells (A,C),  $\beta$ V spectrin is restricted to the hair cells (D). Asterisks indicate positions of the sensory hair cells. (E–I) Isolated hair cells. (E) In IHCs,  $\beta$ V spectrin displays a cytoplasmic staining, with a strong submembrane labeling at the neck region of the cell. (F)  $\beta$ II spectrin is detected in the cuticular plate. (G) In OHCs, the  $\beta$ V spectrin labeling extends all along the lateral wall, similar to that of prestin. (H,I) In these cells, the  $\beta$ II-spectrin subunit predominates in the cuticular plate (H), whereas the  $\alpha$ II subunit is detected in both the cuticular plate and along the lateral wall (I). Scale bars: 5  $\mu$ m.

$\alpha$ II- $\beta$ V spectrin belong to the same molecular complex in OHCs. Therefore,  $\beta$ V spectrin directly interacts with  $\alpha$ II spectrin, band 4.1 protein and F-actin, all of which are essential components of the OHC cortical lattice.

#### $\beta$ V spectrin–prestin interaction

The preferential distribution of  $\beta$ V spectrin at the lateral wall of OHCs (see Fig. 1E,F) suggests that  $\beta$ V spectrin is involved in the electromotility of these cells. The appearance of electromotility in the organ of Corti occurs during a well-defined developmental window (Abe et al., 2007; Marcotti and Kros, 1999). A strict correlation has previously been reported between the onset of and increase in electromotility and the appearance of and increase in prestin immunoreactivity during postnatal maturation of the OHCs in rat (Belyantseva et al., 2000). We thus carried out whole-mount immunofluorescence analyses to study  $\beta$ V spectrin and prestin distributions in the organ of Corti during late-embryonic and postnatal stages in the mouse [embryonic day 18 (E18)–P20] (Fig. 5).  $\beta$ V spectrin labeling within the auditory hair cells was not observed before birth. At E18, however, both the  $\alpha$ II- and  $\beta$ II-spectrin subunits could be detected in IHCs, OHCs and their supporting cells (supplementary material Fig. S2A).  $\beta$ V spectrin labeling at the lateral wall was first detected in the cochlear basal turn at P2 (Fig. 5B,C). In the following days, both the  $\beta$ V spectrin and prestin OHC labeling rapidly progressed towards the cochlear apex (Fig. 5B,C), consistent with the basal-apical gradient of cochlear maturation. A marked increase in the labeling intensities of  $\beta$ V spectrin and prestin occurred between P4 and P8, both along the cochlear partition (Fig.

5C) and within the OHC (Fig. 6B–D). From P12 onwards, the  $\beta$ V spectrin labeling of all OHCs was close to the maximal levels observed in the fully mature OHCs at P20 (Fig. 6A and data not shown). This finding was confirmed by quantifying (see Materials and Methods) relative increases in immunofluorescence intensities for  $\beta$ V spectrin and prestin in OHCs from the apical turn of the cochlea between P2 and P20 (Fig. 6A). Within OHCs,  $\beta$ V spectrin and prestin labeling were first restricted to the tip of the lateral wall, as shown at P3, then progressed downwards so that, by P8, the labeling had extended along the entire length of the lateral wall (Fig. 6B–D). Thus,  $\beta$ V spectrin is recruited to the OHC lateral wall concomitantly with prestin membrane insertion, which itself parallels the maturation of cell electromotility.

Analyses of prestin topology established that the long N and C termini of the transmembrane protein are cytoplasmic (Navaratnam et al., 2005; Zheng et al., 2000). Moreover, a series of short truncations in both cytodomains revealed that, despite normal membrane targeting, these mutations resulted in absent or modified prestin activity both in vitro (Navaratnam et al., 2005; Zheng et al., 2005) and in vivo (Dallos et al., 2008). These functional consequences led the authors to suggest that prestin requires interacting partners to drive OHC motor activity (Navaratnam et al., 2005). We first investigated whether  $\beta$ V spectrin interacts with prestin. A direct interaction could not be detected between full-length  $S^{35}$ -labeled prestin and either GST-tagged  $\beta$ VCH or GST-tagged  $\beta$ VR29 (Fig. 7A). So far, despite many attempts, we have not been able to obtain the full-length cDNA of  $\beta$ V spectrin. The longest cDNA fragment we have isolated and tested for its direct

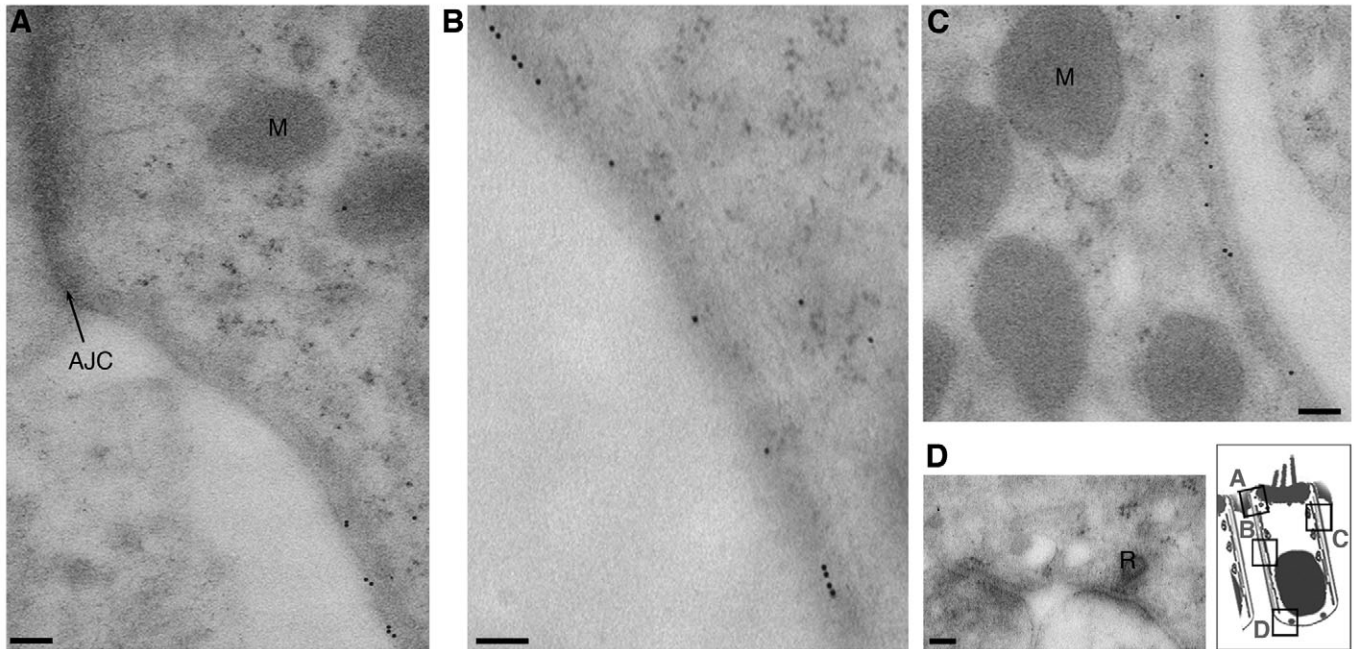


**Fig. 3.** Ultrastructural distribution of βV spectrin in the lateral wall of OHCs. (A-D) βV spectrin immunogold labeling in the lateral wall of a P15 OHC (A-C). Gold particles are not observed at the apical junctional complex (AJC) or in the ribbon (R) synapse area (A,D). M, mitochondria. Scale bars: 100 nm.

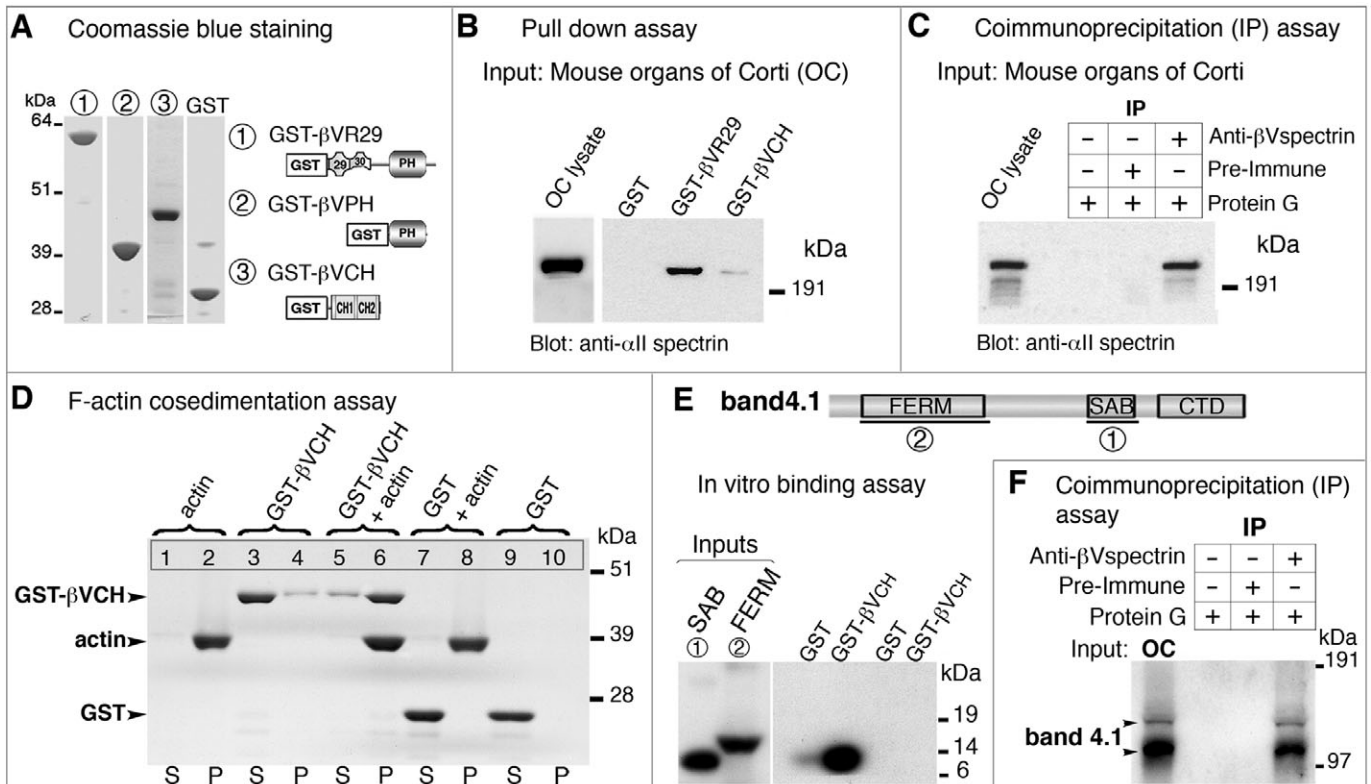


**Fig. 4.** βV spectrin binds to F-actin and forms a complex with αII spectrin and band 4.1 in vivo. (A) GST and GST-tagged βV spectrin fragments used in the binding experiments (Coomassie-blue staining following SDS-PAGE). (B,C) βV spectrin–band-4.1 interaction. The endogenous αII spectrin binds to GST-βVR29 (B) and is immunoprecipitated by the anti-βV spectrin antibody, but not by the preimmune serum or by protein G alone (C). (D) F-actin co-sedimentation assay. The soluble (S) and pellet (P) fractions obtained upon ultracentrifugation are indicated. GST-tagged βVCH is not recovered in the pellet fraction (lane 3). When the same amount of GST-tagged βVCH is incubated with F-actin at 37°C for 30 minutes (lanes 5 and 6), almost all GST-tagged βVCH is recovered with F-actin in the pellet fraction after ultracentrifugation (lane 6). GST alone was used as a negative control (lanes 7-10). (E,F) βV spectrin–band-4.1 interaction. (E) In vitro binding assay. GST-tagged βVCH directly interacts with the SAB domain of band 4.1. (F) Co-immunoprecipitation assay. The anti-βV spectrin antibody immunoprecipitates band 4.1 from lysates of P8 mouse organs of Corti.

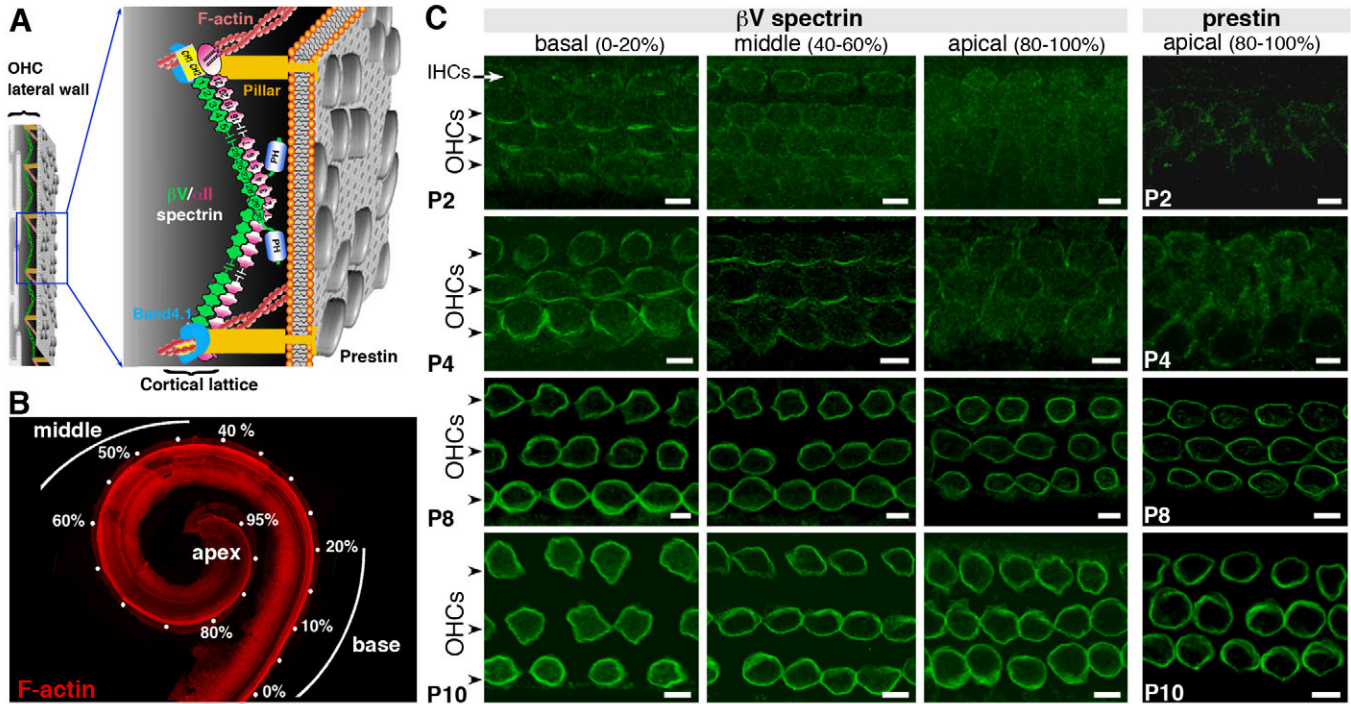


**Fig. 5.** Concomitant time-course distribution of  $\beta$ V spectrin and prestin in OHCs. (A) A model illustrating the role of the  $\alpha$ II- $\beta$ V spectrin network in the OHC lateral wall. The  $\alpha$ II- $\beta$ V spectrin heterotetramers crosslink adjacent circumferential actin filaments, while extending out of the plane (25 nm) to reach the plasma membrane, which is densely packed with the prestin motor protein. (B) An F-actin-labeled cochlea illustrating the different positions (base, middle and apex) along the cochlea longitudinal axis. (C) Whole-mount immunofluorescence analysis of  $\beta$ V spectrin and prestin distributions in the basal (0-20%), middle (40-60%) and apical (80-100%) turns of the cochlea. Consistent with the progressive maturation of the cochlea, the intensities of  $\beta$ V spectrin and prestin stainings in OHCs increase from P2 to P10, and from the basal to the apical zone of the cochlea. Scale bars: 5  $\mu$ m.

interaction with prestin is the  $\beta$ VspecR26 fragment (aa 3012-3674). No interaction was detected between myc-tagged  $\beta$ VspecR26 and GST-tagged prestin-C529 (see Fig. 7E). Although we could not exclude a direct interaction between the long central region of  $\beta$ V spectrin (spectrin repeats 1-25) and prestin, we considered the possibility that an 'intermediary' protein bridges  $\beta$ V spectrin N or C termini to prestin. Because our anti-prestin antibodies failed to immunoprecipitate the native protein, full-length  $S^{35}$ -labeled prestin mixed with protein lysates from adult (P90) mouse organs of Corti were incubated with GST-tagged  $\beta$ VCH, GST-tagged  $\beta$ V29 or GST alone. We found that only GST-tagged  $\beta$ V29 could interact with prestin under these conditions. A binding was not observed with either GST-tagged  $\beta$ VCH or GST alone (Fig. 7B).

To determine which cytoplasmic region of prestin is involved in the  $\beta$ V spectrin-prestin interaction, two different prestin truncated peptides were used (Fig. 7C), i.e. prestin-DelC (aa 1-501) and prestin-C (aa 499-744). In the absence of organ-of-Corti lysates, neither prestin-DelC nor prestin-C bound to GST-tagged  $\beta$ V29 (Fig. 7D). In the presence of organ-of-Corti lysates, however, prestin-C, but not prestin-DelC, did interact with GST-tagged  $\beta$ V29 (Fig. 7D). Also, a GST-tagged  $\beta$ V spectrin fragment containing the PH domain only ( $\beta$ VPH; aa 3531-3643) did interact with both full-length prestin (prestin-FL) and with prestin-C under these conditions (Fig. 7D). This association in the presence of organ-of-Corti lysates was confirmed in the reciprocal experiment, using GST-tagged prestin-C529 (aa 529-744) incubated with detergent extracts prepared from HEK293 cells producing myc-tagged  $\beta$ VCH or myc-tagged  $\beta$ V26 (aa 3012-3674) fusion proteins (Fig. 7E).

The C terminus of the ten different SLC26A family members is the least conserved region of the proteins, suggesting that it is most likely to be responsible for the specific function of each protein (Dorwart et al., 2008; Mount and Romero, 2004). To analyze the specificity of the  $\beta$ V spectrin-prestin interaction, we incubated GST-tagged  $\beta$ V29 with SLC26A4-C, SLC26A5-C (prestin-C), SLC26A6-C or SLC26A7-C cytodomains in the presence of organ-of-Corti extracts. The C terminus of prestin displays only 25-35% aa identity with other SLC26A C termini, including SLC26A4, SLC26A6 or SLC26A7. In the presence of organ-of-Corti lysates, only prestin-C was bound to GST-tagged  $\beta$ V29 (Fig. 8A). Previous reports have shown that some particular amino acid residues in the C-terminal region play a key role in prestin cellular distribution and motor activity (Navaratnam et al., 2005; Zheng et al., 2005). We produced two prestin mutants, Del632 and Del709, which have been shown to impair the ability of prestin to confer non-linear capacitance and motility (Zheng et al., 2005). Del632 lacks the STAS motif (sulphate transporter and anti-sigma factor antagonist domain, aa 633-708), a domain identified in all ten SLC26A proteins. Del709 contains the STAS domain, but lacks the terminal 35 aa of prestin (see Fig. 7C). Neither Del632 nor Del709 became bound to GST-tagged  $\beta$ V29 (Fig. 8B), suggesting that the terminal 35 aa of prestin are necessary for the interaction with  $\beta$ V spectrin in the presence of organ-of-Corti lysates.

Given that the expressions of  $\beta$ V spectrin and prestin vary concomitantly during postnatal stages, we examined the formation of a  $\beta$ V spectrin-prestin complex in the presence of protein extracts derived from P0 (no electromotility), P4, P8 or P35 (fully mature)

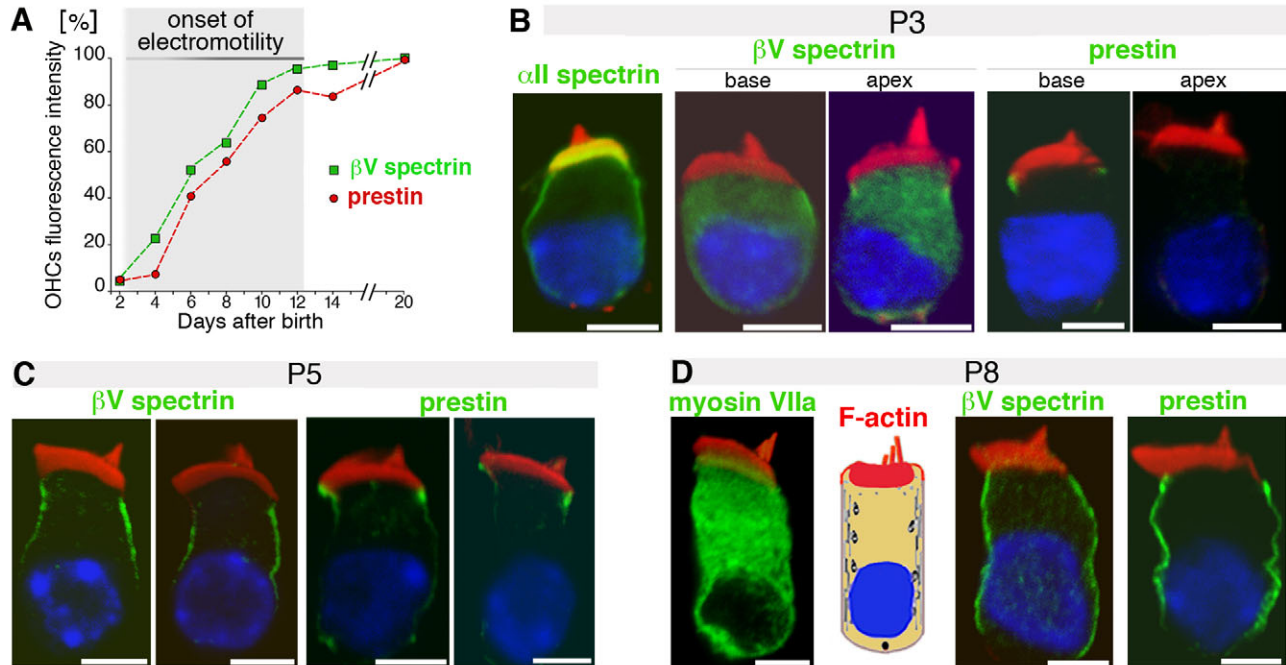


**Fig. 6.** (A) Intensity of OHC immunolabeling with anti- $\beta$ V spectrin (squares) and anti-prestin (circles) antibodies plotted against age (days after birth). The values obtained for the apical turns (80–100%, see Fig. 5B) were averaged, and then normalized to the corresponding average value obtained in P20 mice. (B–D) Parallel distribution of  $\beta$ V spectrin and prestin within differentiating OHCs. (B) At P3, the bulk of  $\beta$ V spectrin staining is diffuse within the cytoplasm. At this stage,  $\alpha$ II spectrin can be detected in the cuticular plate and along the cell lateral wall. In some OHCs from the base of the cochlea, prestin can be detected, essentially at the apico-lateral cell membrane. (C) At P5,  $\beta$ V spectrin and prestin are both detected in the forming cortical lattice. (D) From P8 onwards, the labeling extends along the entire length of the OHC lateral wall. Scale bars: 5  $\mu$ m.

organs of Corti. An interaction between  $\beta$ V spectrin and prestin was not detected when P0 protein extracts were used (Fig. 8C). By contrast, a significant interaction between the two proteins occurred in the presence of P4, P8 or P35 extracts. Furthermore, we could not detect this interaction using protein extracts from the brain, the liver or HEK293 cells, thus suggesting that the  $\beta$ V spectrin–prestin interaction is unlikely to involve a ubiquitous intermediary protein (Fig. 8D). Together, these results led us to conclude that  $\beta$ V spectrin, through its PH domain, can indirectly interact with the C-terminal cytodomain of prestin, via an as yet unknown protein, the expression of which parallels the progressive increase of OHC electromotility.

**Discussion**

In the mammalian cochlea, OHCs act as amplifiers of the sound-induced vibrations of the organ of Corti (Dallos, 1992; Brownell et al., 2001; Ashmore, 2008). Their electromotility is driven by prestin, a motor protein that is present in the lateral wall of OHCs (Zheng et al., 2000; Liberman et al., 2002; Dallos et al., 2008). The seminal studies on the cytomechanics of red blood cells have served as a model system for the development of a large number of experimental, theoretical and computational studies carried out on OHCs to elucidate their lateral-wall mechanical properties (see Brownell et al., 2001; Discher and Carl, 2001; He et al., 2006). Accordingly, the involvement of an actin-spectrin meshwork in sound-induced electromotility was suggested almost 20 years ago (Holley and Ashmore, 1990; Holley et al., 1992). Because we found that  $\beta$ V spectrin is the only  $\beta$  spectrin of the OHC cortical lattice, we conclude that the spectrin network that is localized underneath the OHC lateral wall is based on the  $\beta$ V spectrin subunit, not the expected conventional  $\beta$ II spectrin. In mature OHCs,  $\beta$ V spectrin displays a typical ‘ring’ staining pattern that is restricted to the lateral

wall, where prestin is present. The detection of  $\beta$ V spectrin in the lateral wall of differentiating OHCs strictly parallels that of prestin in the plasma membrane. Moreover, we provide in vitro evidence that  $\beta$ V spectrin, via its PH domain, indirectly interacts with the C-terminal 35 amino acids of prestin, via as yet unknown protein(s). In IHCs, a  $\beta$ V spectrin ‘ring’ staining pattern was observed only in a limited subapical zone (Fig. 2E), a region in which membrane cisternae and pillars similar to those found in the OHC lateral wall have been described (Furness and Hackney, 1990). This suggests the intriguing possibility that the OHC cortical lattice arose from an ancestral structure present in the neck region of auditory hair cells.

The fact that *Drosophila*  $\beta$ -heavy spectrin (Williams et al., 2004), *Caenorhabditis elegans* Sma-1 (McKeown et al., 1998) and mammalian  $\beta$ V spectrin each have independently maintained a 30-repeat length throughout evolution (Stabach and Morrow, 2000), argues in favor of a crucial role for either a longer actin-membrane cross-linker or the need for greater extensible flexibility than can be provided by the other smaller conventional spectrins. The unusually large size of the  $\beta$ V spectrin subunit, and the link between this spectrin and the molecular motor prestin, highlights the need to integrate these data into current models of the OHC electromotile behavior in response to sound stimulation. The main expected function of the  $\alpha$ II- $\beta$ V spectrin network in OHCs is to crosslink actin filaments (see Fig. 5A), providing OHCs with the flexible properties required for lateral-wall contraction-elongation cycles. Nonetheless, considering the  $\beta$ V spectrin interacting partners identified in this study (see supplementary material Fig. S8) and the large number of spectrin repeats for which interacting partners have not yet been identified,  $\beta$ V spectrin might also exert a scaffolding function by clustering and stabilizing submembranous molecular complexes required for normal

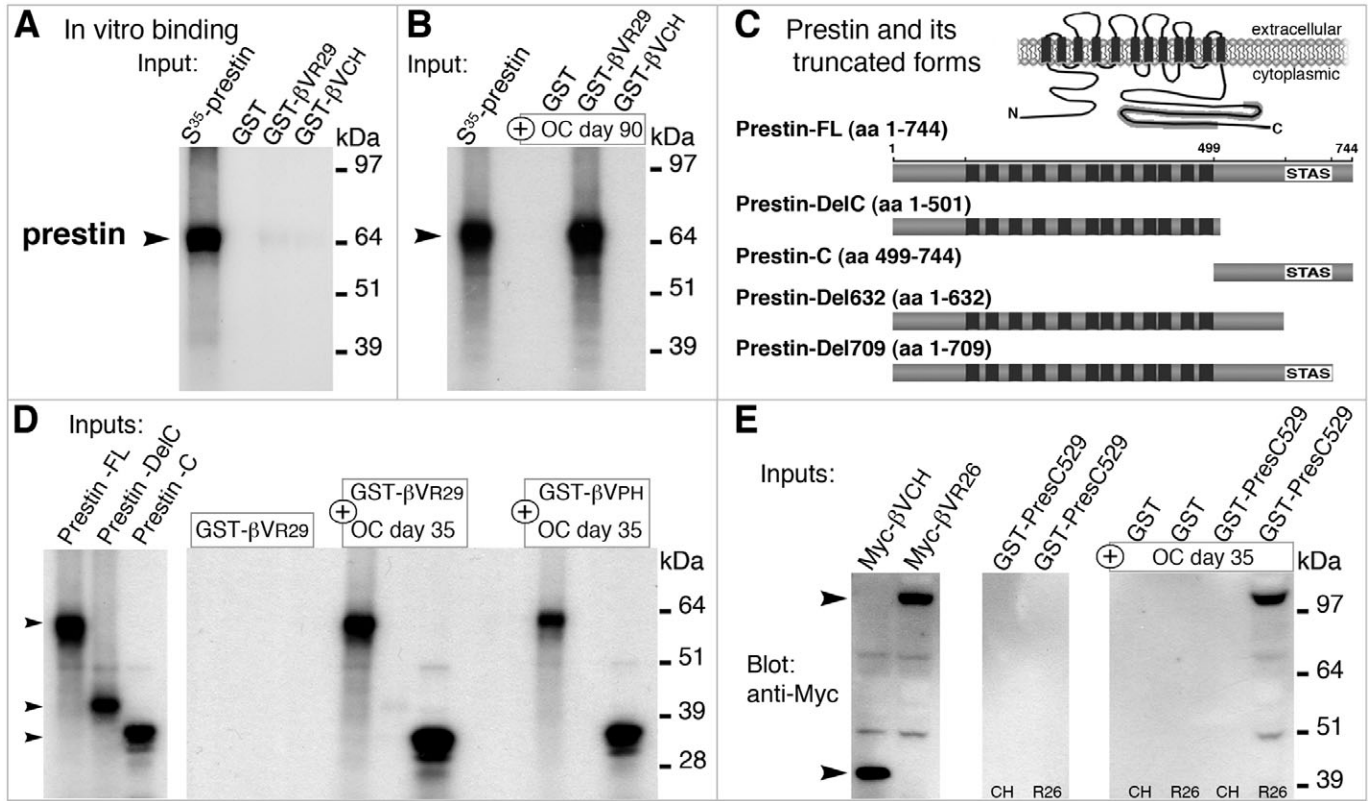


**Fig. 7.**  $\beta$ V spectrin indirectly interacts with prestin. (A,B,D) In vitro binding assays. (A) Neither GST-tagged  $\beta$ VCH nor GST-tagged  $\beta$ VR29 directly interact with full-length prestin. (B) By contrast, the interaction between GST-tagged  $\beta$ VR29 and prestin can be detected when protein extracts derived from P90 organs of Corti (OC) are added to the binding solution. (C-E) Mapping of the  $\beta$ V spectrin-binding region on prestin and of the prestin-binding region on  $\beta$ V spectrin. (C) Schematic diagram of the transmembrane topology of prestin and its deletion constructs used in the pull-down assays. Prestin is a 10- to 12-transmembrane-domain protein, with relatively large cytoplasmic N and C termini. The numbers refer to the corresponding positions of amino acid residues in the rat prestin. (D) In the presence of P35 OC lysates, both the full-length prestin (prestin-FL) and the prestin C-terminal cytoplasmic domain (prestin-C) bind to either GST-tagged  $\beta$ VR29 or GST-tagged  $\beta$ VPH. (E) Western blot. In the reciprocal experiment, GST-tagged prestin-C529 (aa 529-744) binds to the myc-tagged  $\beta$ VR26 (aa 3012-3674) only in the presence of OC lysates.

OHC electromotility. Thanks to the 13 additional spectrin repeats of  $\beta$ V spectrin (30 repeats instead of the 17 repeats found in conventional  $\beta$  spectrins) the  $\alpha$ II- $\beta$ V spectrin crosslinks are long enough to span the gap of ~50-70 nm between adjacent circumferential actin filaments (Holley et al., 1992), while extending out of the plane (25 nm) to the OHC plasma membrane (see Fig. 5A). Notably, the OHC cortical lattice is located ~25 nm beneath the plasma membrane (Holley et al., 1992), a distance that might be too large for conventional spectrins to span. FRAP analysis of lipid mobility in the OHC lateral plasma membrane has shown that diffusion is faster in the longitudinal direction and slower in the circumferential direction (de Monvel et al., 2006; Oghalai et al., 2000). We thus propose that the  $\alpha$ II- $\beta$ V spectrin crosslinks might establish local constraints on the OHC plasma membrane, thereby promoting longitudinal lipid mobility within the plasma membrane while hindering the lateral diffusion of lipids and integral membrane proteins, including prestin.

## Materials and Methods

### Cloning and generation of DNA constructs

PCR-amplified fragments were first cloned into pCR2.1-TOPO (Invitrogen) and their sequences were checked prior to transfer to the appropriate vectors: i.e. pEGFP (Clontech), pCMV-tag3B (myc tag, Stratagene) and pcDNA3 (Invitrogen) for in vitro translation and transfection experiments, and pGEX-4T1 (GST tag, Amersham) for protein production.

For  $\beta$ V spectrin, the  $\beta$ VspecR29 cDNA (aa 3317-3674) was further extended by RACE-PCR using a human Marathon retina cDNA library (Clontech) to obtain the 5' region. The longest cDNA fragment that we isolated was  $\beta$ VspecR26 (aa 3012-3674).  $\beta$ VPH (aa 3531-3643) were reconstituted from the  $\beta$ VspecR29 cDNA. The N-terminal region of  $\beta$ V spectrin,  $\beta$ VCH (aa 1-250), was reconstituted using a P8 mouse inner-ear cDNA library.

The following full-length and cDNA fragments were used: band 4.1G-FERM (aa 214-406) and band 4.1G-SAB (aa 611-678) were reconstituted using the human full-length band 4.1G (Masaki Saito, University of Tohoku, Sendai, Japan). Prestin-C (aa 499-744) and prestin-C529 (aa 529-744) were generated by PCR using full-length rat prestin, prestin-FL (obtained from Bernd Fakler, University of Freiburg, Germany). The C-terminal truncated forms of prestin – DelC (aa 1-501), Del632 (aa 1-632) and Del709 (aa 1-709) – were obtained by introducing stop codons after the indicated positions, using a QuikChange site-directed mutagenesis kit (Stratagene). SLC26A4-C (aa 514-780), SLC26a6-C (aa 487-735) and SLC26A7-C (aa 473-663) were generated by PCR or restriction-enzyme digestion using full-length cDNAs, namely human SLC26A4 (Jonathan Ashmore, University College London, London, UK), mouse SLC26A6 (Shmuel Muallem, University of Texas Southwestern Medical Center, Dallas, TX) and human SLC26A7 (Manoocher Soleimani, University of Cincinnati, Cincinnati, OH), respectively.

### Antibodies and reagents

Two rabbit polyclonal anti- $\beta$ V spectrin antibodies were produced: the anti-h $\beta$ Vp, derived against a human  $\beta$ V spectrin peptide (A36Pep: AQLAETRDPAQAKG; aa 3519-3532), and the anti-h $\beta$ Vrec, derived against a human  $\beta$ V spectrin fusion protein (aa 3443-3668). The specificity of the purified antibodies was checked by immunofluorescence and immunoblot analysis (see supplementary material Fig. S3A-D). The anti-h $\beta$ Vrec, referred to as anti- $\beta$ V spectrin antibody, was used in all the immunofluorescence and immunoprecipitation experiments. The following additional antibodies and reagents were used: anti-neurofilament-2, anti- $\beta$ III-tubulin, anti-GST (Amersham), and anti-GFP (Clontech). Anti- $\beta$ I-spectrin (NCL-SEPC2, Novocastra),

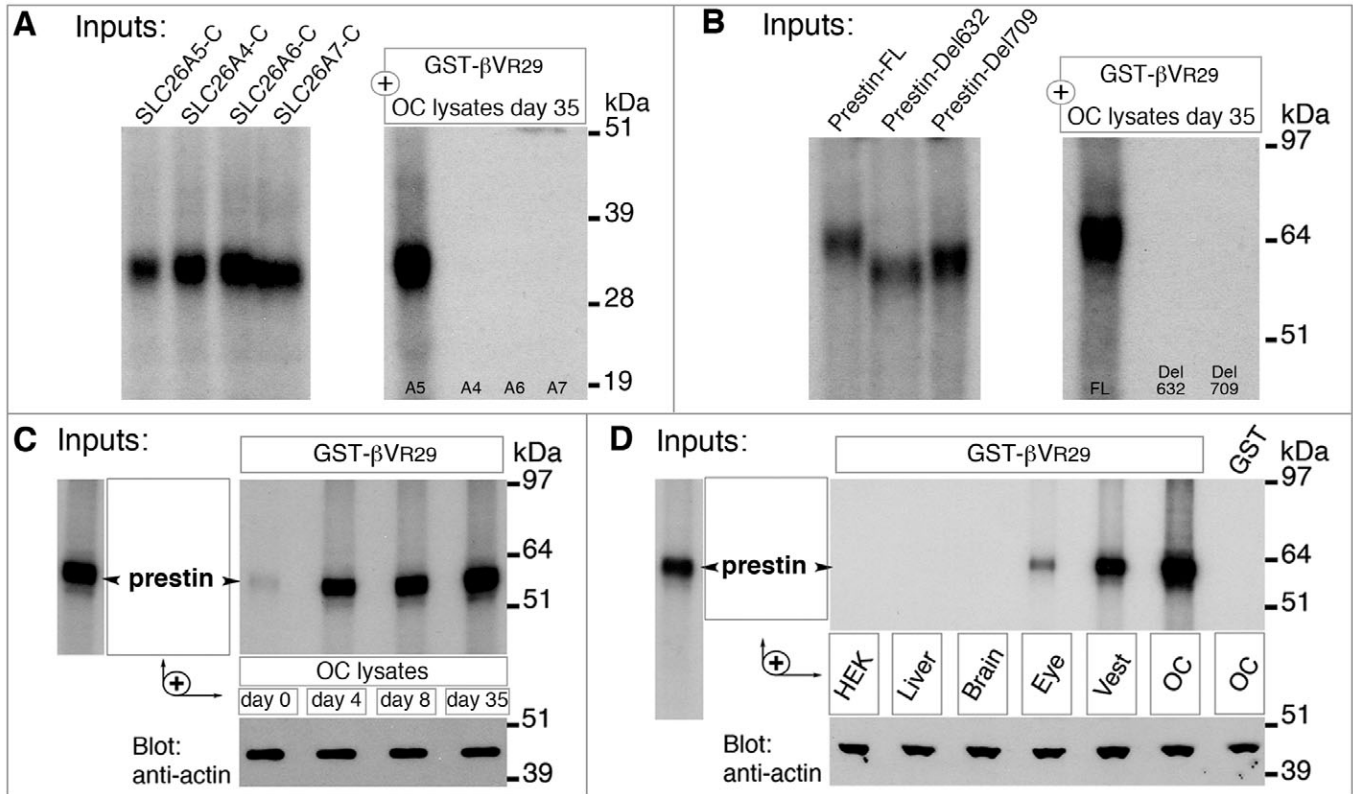


**Fig. 8.** Specificity, time and spatial dependency of the βV spectrin–prestin association. (A) In the presence of OC lysates, only SLC26A5-C (prestin-C), but not SLC26A4-C (pendrin-C), SLC26A6-C or SLC26A7-C, binds to GST-tagged βVR29. (B) This interaction cannot be detected when prestin-FL lacks either the STAS domain (Del632) or the last 35 amino acid residues (Del709). (C) In the presence of protein extracts derived from P0 organs of Corti (a stage at which OHC electromotility is not yet present), prestin does not associate with GST-tagged βVR29. The interaction can be seen only when lysates from P4, P8 or P35 organs of Corti are used. (D) βV spectrin–prestin interaction in the presence of different mouse tissue lysates. An interaction cannot be detected when using lysates derived from the brain, liver or HEK293 cells. Vest, vestibule (balance organ). The same amounts of proteins were used at each developmental stage, as shown by western blot analysis of the lysates with an anti-actin antibody (C,D).

mouse anti-βII-spectrin (BD), rabbit anti-band-4.1G, goat anti-βIII-spectrin, goat anti-prestin, and mouse anti-myc (clone 9E10) antibodies were obtained from Santa Cruz Biotechnology. Anti-αII-spectrin (Nicolas et al., 2002) and anti-βIV spectrin (Yang et al., 2004) antibodies were obtained from Gaël Nicolas (Institut National de la Transfusion Sanguine, Paris, France) and Matthew N. Rasband (University of Connecticut, CT), respectively. The anti-myosin-VIIa antibody was used as previously described (El-Amraoui et al., 1996). TRITC-phalloidin (Sigma) and DAPI (1 μg/ml, Sigma) were used to label F-actin and cell nuclei, respectively.

**Protein-protein interaction assays**

GST proteins were produced in *E. coli* and purified using glutathione Sepharose 4B. Equal amounts of either fusion proteins or GST alone were used for in vitro binding assays as described (Kussel-Andermann et al., 2000a). Radiolabeled proteins were translated in vitro with the T7/T3-coupled transcription-translation system (Promega) according to the manufacturer’s instructions.

**In vitro binding assays**

Briefly, to test the βV spectrin–prestin direct interaction, a bacterial lysate containing GST-βVR29, GST-βVCH or GST alone was incubated with pre-equilibrated glutathione-Sepharose beads for 90 minutes at 4°C. The agarose-conjugated beads were washed three times with binding buffer (5% glycerol, 5 mM MgCl<sub>2</sub> and 0.1% Triton X-100 in phosphate-buffered saline) supplemented with a protease-inhibitor cocktail (Roche), and then incubated with the in vitro translated <sup>35</sup>S-labeled prestin for 3 hours at 4°C on a rotating wheel. For βVspecR29-prestin indirect association, the <sup>35</sup>S-labeled prestin, either full length (FL) or the different truncation mutants (DelC, C, Del632, or Del709), was equally divided between the samples. Equal amounts of HEK293 cells or tissue extracts were also added in each of the binding reactions prior to incubation with the immobilized GST-tagged fusion proteins at 4°C for 3 hours. The conjugated beads were then washed four times with the binding buffer supplemented with 150 mM NaCl. Bound proteins were resuspended in 30 μl 2× concentrated SDS sample buffer and analyzed on 4-12% or 4-16% SDS-polyacrylamide gels (Invitrogen). The gel was stained with Coomassie blue, dried and processed for autoradiography.

**GST pull-down and co-immunoprecipitation experiments**

Lysates derived from human embryonic kidney HEK293 cells or from the different mouse tissues were used. HEK293 cells were transfected using Lipofectamine 2000 (Invitrogen) according to the manufacturer’s instructions. The HEK pellets and mouse tissues were solubilized by sonication in 500 μl of the immunoprecipitation buffer [150 mM NaCl, 50 mM Tris-HCl, pH 7.5, 500 μM EDTA, 100 μM EGTA, 0.1% SDS, 1% Triton-X100, and 1% sodium deoxycholate, complemented with an EDTA-free cocktail of protease inhibitors (Roche)]. The resulting lysates were cleared via a 15,000 g centrifugation step at 4°C for 45 minutes. The soluble fraction was incubated with the appropriate agarose-conjugated beads for 3 hours at 4°C. For the co-immunoprecipitation assay, the soluble fraction was incubated for 6 hours either with the antibody against βV spectrin, the pre-immune serum or immunoprecipitation buffer alone, then with 50 μl of pre-equilibrated protein G at 4°C overnight. After three to four washes with immunoprecipitation buffer, bound proteins were resuspended in 30 μl 2× concentrated SDS sample buffer and analyzed on a 4-12% SDS-polyacrylamide gel (Invitrogen) followed by western blot using the appropriate antibodies. Horseradish peroxidase (HRP)-conjugated goat anti-rabbit antibodies (Bio-Rad) and the ECL chemiluminescence system (Amersham) were used for detection.

**Actin binding assays**

A 50 μM G-actin solution (Molecular Probes) was polymerized by incubation for 30 minutes at 37°C in a high-salt buffer (10 mM Tris pH 8.0; 50 mM KCl; 2 mM MgCl<sub>2</sub>; 0.2 mM CaCl<sub>2</sub>; 0.2 mM ATP; 0.5 mM DTT). Co-sedimentation assays were done by incubating 8 μg of either GST-βVCH or GST, with 20 μl of 17 μM F-actin solution for 1 hour at 37°C with agitation, followed by ultracentrifugation (150,000 g, 1 hour).

**Hair-cell-isolation, immunofluorescence and electron-microscopy analyses**

Mice were killed according to Institut Pasteur guidelines for animal use. For hair-cell isolation, mice were anesthetized with CO<sub>2</sub> inhalation and then decapitated. The inner ears were rapidly removed and strips of the organ of Corti or vestibular sensory epithelia were microdissected in standard saline solution (110 mM NaCl, 2 mM KCl,

4 mM CaCl<sub>2</sub>, 2 mM MgCl<sub>2</sub>, 3 mM D-glucose and 10 mM HEPES, pH 7.25); osmolarity was adjusted to 325±2 mOsm with glucose. After 5 minutes of incubation in 1 mg/ml collagenase type IV (Sigma), cells were dissociated by gentle reflux of the tissue through the needle of a Hamilton syringe (N. 705, 22 gauge). Cells were allowed to settle for 20 minutes on a glass-bottom Petri dish (MatTek) coated with CellTak. Upon fixation with paraformaldehyde 4% for 30 minutes, they were proceeded for immunohistochemistry as described (Kussel-Andermann et al., 2000a; Kussel-Andermann et al., 2000b). Secondary antibodies (Invitrogen) were as follows: Alexa-Fluor-488-conjugated goat anti-rabbit, Alexa-Fluor-488-conjugated donkey anti-goat and Cy3-anti-mouse.

Images were collected using a laser scanning confocal microscope (LSM540; Zeiss) equipped with a plan Apo 63× NA 1.4 oil-immersion-objective lens. Images to be quantified were acquired at 2-μm increments with pinholes open to obtain optical sections of 2-μm thick. Image sets to be compared were acquired during the same session and using the same acquisition settings. Background intensities were equalized to a similar level in all images. Equally sized areas from the apical turn of at least three cochleas were analyzed using an LSM540 software to estimate the fluorescence associated to OHCs. For each stage, five z-confocal sections through OHCs (section 1 is at the level of the cuticular plate) were assembled and the fluorescence intensities of equal square areas containing approximately four OHCs were measured.

Post-embedding immunogold electron microscopy was performed on P15 organs of Corti as described (Roux et al., 2006) (and references therein). The cochleas were fixed in 4% paraformaldehyde and 0.2% glutaraldehyde in PBS pH 7.4, by perfusion through the oval and round windows. The organs of Corti were microdissected and immersed in the same fixative solution for 2 hours at 4°C. After four washes in PBS, the samples were processed according to the progressive-lowering-of-temperature technique. A 15-nm gold-conjugated rabbit anti-goat IgG (Tebu) was used.

We are grateful to Jean-Pierre Hardelin for critical reading of this manuscript, and to Jonathan Ashmore and Dominik Oliver for their comments. We thank Gaël Nicolas, Bernd Fakler, Matthew Rasband, Masaki Saito, Jonathan Ashmore, Shmuel Muallem and Manoocher Soleimani for reagents, and Isabelle Perfettini for technical assistance. All images were acquired using the Institut Pasteur PFID facility. This work was supported by Fonds MAZET-DANET (Fondation de France) and ANR-07-MRARE-009-01 to A.E., and grants from 'Sesame-Ile de France', R. & G. Strittmatter Foundation and from the European Commission FP6 Integrated Project EuroHear LSHG-CT-2004-512063 to C.P. K.L. is a recipient of a doctoral fellowship from the MENRT.

## References

- Abe, T., Kakehata, S., Kitani, R., Maruya, S., Navaratnam, D., Santos-Sacchi, J. and Shinkawa, H. (2007). Developmental expression of the outer hair cell motor prestin in the mouse. *J. Membr. Biol.* **215**, 49-56.
- Adachi, M. and Iwasa, K. H. (1997). Effect of diamide on force generation and axial stiffness of the cochlear outer hair cell. *Biophys. J.* **73**, 2809-2818.
- Ashmore, J. (2008). Cochlear outer hair cell motility. *Physiol. Rev.* **88**, 173-210.
- Belyantseva, I. A., Adler, H. J., Curi, R., Frolenkov, G. I. and Kachar, B. (2000). Expression and localization of prestin and the sugar transporter GLUT-5 during development of electromotility in cochlear outer hair cells. *J. Neurosci.* **20**, RC116.
- Bretscher, A., Edwards, K. and Fehon, R. G. (2002). ERM proteins and merlin: integrators at the cell cortex. *Nat. Rev. Mol. Cell. Biol.* **3**, 586-599.
- Brownell, W. E., Bader, C. R., Bertrand, D. and de Ribaupierre, Y. (1985). Evoked mechanical responses of isolated cochlear outer hair cells. *Science* **227**, 194-196.
- Brownell, W. E., Spector, A. A., Raphael, R. M. and Popel, A. S. (2001). Micro- and nanomechanics of the cochlear outer hair cell. *Annu. Rev. Biomed. Eng.* **3**, 169-194.
- Chan, D. K. and Hudspeth, A. J. (2005). Ca<sup>2+</sup> current-driven nonlinear amplification by the mammalian cochlea in vitro. *Nat. Neurosci.* **8**, 149-155.
- Dallos, P. (1992). The active cochlea. *J. Neurosci.* **12**, 4575-4585.
- Dallos, P., Wu, X., Cheatham, M. A., Gao, J., Zheng, J., Anderson, C. T., Jia, S., Wang, X., Cheng, W. H., Sengupta, S. et al. (2008). Prestin-based outer hair cell motility is necessary for mammalian cochlear amplification. *Neuron* **58**, 333-339.
- De Matteis, M. A. and Morrow, J. S. (2000). Spectrin tethers and mesh in the biosynthetic pathway. *J. Cell Sci.* **113**, 2331-2343.
- de Monvel, J. B., Brownell, W. E. and Ulfendahl, M. (2006). Lateral diffusion anisotropy and membrane lipid/skeleton interaction in outer hair cells. *Biophys. J.* **91**, 364-381.
- Discher, D. E. and Carl, P. (2001). New insights into red cell network structure, elasticity, and spectrin unfolding – a current review. *Cell Mol. Biol. Lett.* **6**, 593-606.
- Dorwart, M. R., Shcheynikov, N., Yang, D. and Muallem, S. (2008). The solute carrier 26 family of proteins in epithelial ion transport. *Physiology (Bethesda)* **23**, 104-114.
- Dubreuil, R. R. (2006). Functional links between membrane transport and the spectrin cytoskeleton. *J. Membr. Biol.* **211**, 151-161.
- El-Amraoui, A., Sahly, I., Picaud, S., Sahel, J., Abitbol, M. and Petit, C. (1996). Human Usher IB/mouse *shaker-1*; the retinal phenotype discrepancy explained by the presence/absence of myosin VIIA in the photoreceptor cells. *Hum. Mol. Genet.* **5**, 1171-1178.
- Fettiplace, R. (2006). Active hair bundle movements in auditory hair cells. *J. Physiol.* **576**, 29-36.
- Furness, D. N. and Hackney, C. M. (1990). Comparative ultrastructure of subsurface cisternae in inner and outer hair cells of the guinea pig cochlea. *Eur. Arch. Otorhinolaryngol.* **247**, 12-15.
- He, D. Z., Zheng, J., Kalinec, F., Kakehata, S. and Santos-Sacchi, J. (2006). Tuning in to the amazing outer hair cell: membrane wizardry with a twist and shout. *J. Membr. Biol.* **209**, 119-134.
- Holley, M. C. and Ashmore, J. F. (1988). A cytoskeletal spring in cochlear outer hair cells. *Nature* **335**, 635-637.
- Holley, M. C. and Ashmore, J. F. (1990). Spectrin, actin and the structure of the cortical lattice in mammalian cochlear outer hair cells. *J. Cell Sci.* **96**, 283-291.
- Holley, M. C., Kalinec, F. and Kachar, B. (1992). Structure of the cortical cytoskeleton in mammalian outer hair cells. *J. Cell Sci.* **102**, 569-580.
- Kennedy, S. P., Warren, S. L., Forget, B. G. and Morrow, J. S. (1991). Ankyrin binds to the 15th repetitive unit of erythroid and nonerythroid beta-spectrin. *J. Cell Biol.* **115**, 267-277.
- Knipper, M., Zimmermann, U., Kopschall, I., Rohbock, K., Jungling, S. and Zenner, H. P. (1995). Immunological identification of candidate proteins involved in regulating active shape changes of outer hair cells. *Hear. Res.* **86**, 100-110.
- Kussel-Andermann, P., El-Amraoui, A., Saffiedine, S., Hardelin, J. P., Nouaille, S., Camonis, J. and Petit, C. (2000a). Unconventional myosin VIIA is a novel A-kinase-anchoring protein. *J. Biol. Chem.* **275**, 29654-29659.
- Kussel-Andermann, P., El-Amraoui, A., Saffiedine, S., Nouaille, S., Perfettini, I., Lecuit, M., Cossart, P., Wolfrum, U. and Petit, C. (2000b). Vezatin, a novel transmembrane protein, bridges myosin VIIA to the cadherin-catenins complex. *EMBO J.* **19**, 6020-6029.
- Liberman, M. C., Gao, J., He, D. Z., Wu, X., Jia, S. and Zuo, J. (2002). Prestin is required for electromotility of the outer hair cell and for the cochlear amplifier. *Nature* **419**, 300-304.
- Mahendrasingam, S., Furness, D. N. and Hackney, C. M. (1998). Ultrastructural localisation of spectrin in sensory and supporting cells of guinea-pig organ of Corti. *Hear. Res.* **126**, 151-160.
- Marcotti, W. and Kros, C. J. (1999). Developmental expression of the potassium current I<sub>K,n</sub> contributes to maturation of mouse outer hair cells. *J. Physiol.* **520**, 653-660.
- Markin, V. S. and Kozlov, M. M. (1988). Mechanical properties of the red cell membrane skeleton: analysis of axisymmetric deformations. *J. Theor. Biol.* **133**, 147-167.
- McKeown, C., Praitis, V. and Austin, J. (1998). Sma-1 encodes a betaH-spectrin homolog required for *Caenorhabditis elegans* morphogenesis. *Development* **125**, 2087-2098.
- Mount, D. B. and Romero, M. F. (2004). The SLC26 gene family of multifunctional anion exchangers. *Pflugers Arch.* **447**, 710-721.
- Navaratnam, D., Bai, J. P., Samaranyake, H. and Santos-Sacchi, J. (2005). N-terminal-mediated homomultimerization of prestin, the outer hair cell motor protein. *Biophys. J.* **89**, 3345-3352.
- Nicolas, G., Fournier, C. M., Galand, C., Malbert-Colas, L., Bournier, O., Kroviarski, Y., Bourgeois, M., Camonis, J. H., Dhermy, D., Grandchamp, B. et al. (2002). Tyrosine phosphorylation regulates alpha II spectrin cleavage by calpain. *Mol. Cell. Biol.* **22**, 3527-3536.
- Oghalai, J. S., Patel, A. A., Nakagawa, T. and Brownell, W. E. (1998). Fluorescence-imaged microdeformation of the outer hair cell lateral wall. *J. Neurosci.* **18**, 48-58.
- Oghalai, J. S., Zhao, H. B., Kutz, J. W. and Brownell, W. E. (2000). Voltage- and tension-dependent lipid mobility in the outer hair cell plasma membrane. *Science* **287**, 658-661.
- Roux, I., Saffiedine, S., Nouvian, R., Grati, M., Simmler, M. C., Bahloul, A., Perfettini, I., Le Gall, M., Rostaing, P., Hamard, G. et al. (2006). Otoferlin, defective in a human deafness form, is essential for exocytosis at the auditory ribbon synapse. *Cell* **127**, 277-289.
- Stabach, P. R. and Morrow, J. S. (2000). Identification and characterization of beta V spectrin, a mammalian ortholog of *Drosophila* beta H spectrin. *J. Biol. Chem.* **275**, 21385-21395.
- Williams, J. A., MacIver, B., Klipfell, E. A. and Thomas, G. H. (2004). The C-terminal domain of *Drosophila* (beta) heavy-spectrin exhibits autonomous membrane association and modulates membrane area. *J. Cell Sci.* **117**, 771-782.
- Yang, Y., Lacas-Gervais, S., Morest, D. K., Solimena, M. and Rasband, M. N. (2004). BetaIV spectrins are essential for membrane stability and the molecular organization of nodes of Ranvier. *J. Neurosci.* **24**, 7230-7240.
- Zhang, M., Kalinec, G. M., Urrutia, R., Billadeau, D. D. and Kalinec, F. (2003). ROCK-dependent and ROCK-independent control of cochlear outer hair cell electromotility. *J. Biol. Chem.* **278**, 35644-35650.
- Zheng, J., Shen, W., He, D. Z., Long, K. B., Madison, L. D. and Dallos, P. (2000). Prestin is the motor protein of cochlear outer hair cells. *Nature* **405**, 149-155.
- Zheng, J., Du, G. G., Matsuda, K., Orem, A., Aguinaga, S., Deak, L., Navarrete, E., Madison, L. D. and Dallos, P. (2005). The C-terminus of prestin influences nonlinear capacitance and plasma membrane targeting. *J. Cell Sci.* **118**, 2987-2996.
- Zine, A. and Schweitzer, L. (1997). Localization of proteins associated with the outer hair cell plasma membrane in the gerbil cochlea. *Neuroscience* **80**, 1247-1254.